

Article

Not peer-reviewed version

Effect of Material, Number of Yarns and Loop Length on Pressure, Stretchability and Thermal Properties of Seamless Knitted Fabrics for Compression Textiles

[Nga Wun Li](#)^{*}, [Mei-ying Kwan](#), [Kit-lun Yick](#)

Posted Date: 2 March 2026

doi: 10.20944/preprints202603.0050.v1

Keywords: pressure; extension; thermal comfort; loop length; seamless knitting; compression textiles



Preprints.org is a free multidisciplinary platform providing preprint service that is dedicated to making early versions of research outputs permanently available and citable. Preprints posted at Preprints.org appear in Web of Science, Crossref, Google Scholar, Scilit, Europe PMC.

Copyright: This open access article is published under a [Creative Commons CC BY 4.0 license](#), which permit the free download, distribution, and reuse, provided that the author and preprint are cited in any reuse.

Disclaimer/Publisher's Note: The statements, opinions, and data contained in all publications are solely those of the individual author(s) and contributor(s) and not of MDPI and/or the editor(s). MDPI and/or the editor(s) disclaim responsibility for any injury to people or property resulting from any ideas, methods, instructions, or products referred to in the content.

Article

Effect of Material, Number of Yarns and Loop Length on Pressure, Stretchability and Thermal Properties of Seamless Knitted Fabrics for Compression Textiles

Nga Wun Li ^{1,*}, Mei-ying Kwan ² and Kit-lun Yick ²

¹ Faculty of Design and Society, University of Technology Sydney, Broadway, NSW 2007, Australia

² School of Fashion and Textiles, The Hong Kong Polytechnic University, Hung Hom, Kowloon, Hong Kong

* Correspondence: ngawun.li@uts.edu.au

Abstract

Compression textiles have been widely applied in medical, sportswear, and daily usage, with single-jersey structures produced by circular knitting dominating the market due to their thinness and light weight. However, the presence of seams may compromise compression performance and wearer comfort. This study investigates the effects of yarn material, number of yarns, and loop length on pressure, stretchability, and thermal comfort of seamless punch-lace knitted fabrics and explores their potential application in compression textiles. The results show that yarn number is the dominant factor influencing fabric stiffness, stretchability, and pressure. Fabrics with increased yarn content demonstrate higher maximum load and compression pressure. Smaller loop lengths and additional reinforcing yarns improve dimensional stability and resistance to extension. Air permeability decreases with increasing yarn number due to increased fabric thickness and reduced porosity, while thermal conductivity increases and is positively associated with ventilation resistance, indicating a trade-off between heat transfer and breathability. Surface friction and roughness are significantly affected by yarn number, yarn material, and loop length, whereas water vapour permeability shows no significant relationship with the investigated variables. Overall, seamless punch lace knitted fabrics demonstrate strong potential for compression applications, although careful design is required to balance breathability and thermal comfort.

Keywords: pressure; extension; thermal comfort; loop length; seamless knitting; compression textiles

1. Introduction

Compression textiles have been widely applied in the medical sector for many decades as a first-line treatment for a range of venous diseases [1]. The underlying compression mechanism involves applying the highest pressure at the ankles to create a graduated pressure profile that gradually decreases toward the knees, thereby assisting blood flow upward toward the heart [2,3] and improving venous circulation in the lower limbs. Owing to their demonstrated benefits in medical contexts, compression textiles have increasingly been adopted in leisure, sports, and everyday wellness applications, such as travel socks [4]. Previous studies have suggested that sports compression garments can positively influence muscle fatigue indicators and perceived muscle soreness during post-exercise recovery [5,6], increase venous return and muscle blood flow, improve muscle oxygenation during rest periods [7], prevent injury recurrence, and reduce symptoms of existing sports injuries [8]. However, inconsistent findings regarding the effectiveness of compression garments in enhancing sports performance and recovery have been reported across the literature [9,10]. These discrepancies may be attributed to limited consideration of garment-related factors, such as fabric properties, garment design, and construction, as well as heterogeneity in experimental protocols [4,10].

Circular and flatbed weft-knitting technologies are widely used in the production of elastic compression textiles [11,12]. However, both technologies typically produce garments with seams, which can lead to uneven pressure distribution and potentially compromise the effectiveness of compression therapy and wearer comfort. Single-jersey structures are commonly employed in circular knitting to produce lightweight compression stockings with plain colours. They are frequently used in medical compression stockings, where aesthetic requirements are relatively low. Circular knitting can produce stockings without side seams along the leg, although seams remain in other areas, such as the stocking head. In sports applications, flatbed weft-knitted compression stockings are available in a variety of structures, including single and double jersey, interlock, rib, and spacer fabrics, often incorporating elastic yarns through inlay or plating techniques [12,13]. These structures offer greater visual variety, enabling diverse colours and patterns that enhance the attractiveness of sports apparel. However, they may also increase fabric thickness and weight, reduce breathability, and raise production costs. Consequently, single-coloured compression stockings continue to dominate the market. Despite this, the integration of graphical patterns into compression textiles using seamless knitting technology remains largely unexplored.

Seamless weft-knitting technology enables made-to-measure production, which is particularly advantageous for compression garments, where precise fit is essential for optimal performance. Recent advancements in the Shima Seiki SWG-XR seamless knitting machine have expanded the capability to produce graphical patterns, such as punch lace knitted structures, offering new opportunities to enhance both the functionality and aesthetics of compression textiles. The yarn selection and structural design of textiles directly influence their pressure characteristics and fabric properties, thereby affecting garment efficacy, user comfort, and compliance. Various weft-knitted structures, including rib, single jersey, piqué, and inlaid knits, have been used in the construction of compression textiles [12,14]. Previous research has shown that plaited knit structures with larger loop lengths allow greater extensibility but produce lower compression [15]. Increased fabric thickness, stitch density, and fabric weight, together with reduced transverse elasticity, are associated with higher pressure [16]. Lower fabric thickness and weight contribute to improved comfort [14], while higher spacer yarn density enhances air permeability [17]. Our recent studies demonstrated that the pressure and thermal conductivity of punch lace knitted fabrics are significantly influenced by yarn number and material, but not by the knitted pattern itself [18]. Nevertheless, research on how other knitting parameters affect the textile properties of punch lace structures remains limited. Therefore, this study systematically analyses the influence of fabric structural parameters on pressure, stretchability, permeability, thermal conductivity, and surface performance. The findings provide valuable insights for the design and development of compression textiles and contribute to advancements in textile-based compression apparel.

2. Materials and Methods

2.1. Fabrication of Knitted Samples

Four types of yarn were used, including (A) 43D 69% Nylon 31% Lycra, (B) 90D 86% Nylon 14% Spandex, (C) 94dtex 80% Polyamide 6.6 20% Lycra, and (D) 25D 77% Nylon 23% Spandex.

Seven seamless knitted fabric samples with various numbers of yarn, loop length and yarn material were fabricated in a punch lace knitted structure, and one knitted fabric in single jersey structure was produced as the control. All samples were knitted on an 18-gauge seamless knitting machine (SWG-XR, SHIMA SEIKI, Japan).

The punch lace structure was produced using two different yarns knitted simultaneously: the main yarn formed knitted loops on all needles, while the auxiliary yarn formed knitted loops on two selected needles and float stitches across the remaining five needles in a repeating pattern. All samples were produced using identical knitting parameters and knitted in tubular form, with a height of 10 cm and a width of 6.5 cm. Two specimens were prepared for each knitting condition. Details of the experimental design, fabric composition, and sample specifications are provided in Tables 1–3.

Table 1. Design of experiment.

Factor	Level							
Number of yarns	2		4		5		5.5	
Loop length	4.6		5		5.5		5.5	
Yarn material	A) 43D	69%	B) 90D	86% nylon	C) 94dtex	80%	D) 25D	77%
	Nylon	31%	14% spandex		Polyamide	6.6	Nylon	23%
	Lycra				20% Lycra		spandex	

Table 2. Fabric component.

Fabric component	L1-L3	S1-S2	S3
Main yarn (without float)	Yarn C	Yarn C	Yarn C
Auxiliary yarn (with float)	Yarn A	Yarn B	Yarn D

Knitting notations of punch lace structure

Legend:
○ Main yarn (without float)
○ Auxiliary yarn (with float)

Table 3. Sample specifications of punch lace knitted specimens and control fabric.

Fabric code	Number of yarns				Loop length	Weight/unit area (g/m ²)	Thickness (mm)	Microscopic view of fabric	
	Yarn A	Yarn B	Yarn C	Yarn D				Front	Back
L1	2	/	2	/	5.50	266.12	1.27		
L2	2	/	4	/	5.50	337.96	1.53		
L3	2	/	4	/	5.00	335.51	1.52		
L4	2	/	4	/	4.60	325.71	1.54		
S1	/	2	2	/	5.20	343.67	1.49		
S2	/	2	4	/	5.20	452.24	1.77		
S3	/	/	2	2	5.50	270.20	1.39		
Control	/	/	2	/	5.20	242.45	1.00		

2.2. Evaluation of Fabrics

The properties of the knitted samples were evaluated according to relevant textile standards (Table 4). The pressure exerted by the tubular knitted samples was measured using an AMI air-pack pressure sensor (AMI3037-SB-SET, SANKO TSUSHO CO., LTD., Japan) at the ankle position of a 3D-printed leg mannequin. A thin sensor bladder with a thickness of 1 mm and a diameter of 20 mm was used for the measurements (Figure 1).

The leg mannequin, with an ankle circumference of 21 cm and a calf circumference of 33.5 cm [19], was printed using a BigRep ONE printer with polylactic acid (PLA) and covered with a 1 mm thick Pevalen™ prosthetic cover (Embreis, Sweden).

Stretchability tests were conducted to assess fabric elasticity and recovery, which are critical for garment fit and durability. The maximum load at 50% extension was measured, representing the force required to stretch the fabric to 50% of its initial length; higher maximum load values indicate greater fabric stiffness. Fabric growth after 50% extension was measured according to ASTM D3107. A higher fabric growth (%) indicates a greater permanent change in fabric length after the removal of tensile stress.

Thermal properties, including thermal conductivity and water vapour transmission, were measured to evaluate wearer comfort. Thermal conductivity represents the rate of heat transfer through the sample due to a temperature gradient, while water vapour transmission assesses moisture permeability over a 24-hour period. Surface friction and roughness tests were also conducted to determine surface irregularities and resistance to sliding against another material, which are important indicators of fabric hand feel and comfort.

Prior to testing, all fabric samples were conditioned for 24 hours at a temperature of 20 ± 1 °C and a relative humidity of $65\% \pm 5\%$. Two samples were produced for each fabric type. Each sample was tested three to six times at different locations, and the mean values were calculated and reported.

Table 4. Summary of test methods.

Property	Test parameter	Device	Testing Standard
Thickness	Thickness under pressure	Thickness gauge (Model BC1110-1-04, AMES LOGIC Basic, USA)	ASTM D1777 Standard Test Method for Thickness of Textile Materials
Pressure	Pressure	Leg mannequin with an AMI air-pack pressure sensor (AMI3037-SB-SET, SANKO TSUSHO CO., LTD, Japan)	CEN/TF 15831 Method for testing compression in medical hosiery
Stretchability	Load, strain	5566 tensile tester (Instron®, US)	EN 14704 Determination of the elasticity of fabrics
Air permeability	Ventilation resistance	Air permeability tester (KES-F8-AP1, KATO Tech Co. Ltd., Japan)	ASTM-D737-18 Standard Test Method for Air Permeability of Textile Fabrics
Thermal comfort	Water vapor transmission rate	Water Vapour Permeability Tester	ASTM E96 Standard Test Methods for Water Vapor Transmission of Materials
	Thermal conductivity	Thermal measuring unit (KES-F7 Thermo Labo II, KATO Tech Co., Ltd., Japan)	JIS L 1927 Standard Test for Textiles-Measurement method of cool touch feeling property
Surface	Surface roughness, surface friction	KES-FB4-A Surface Tester	JIS B0601 Surface Roughness

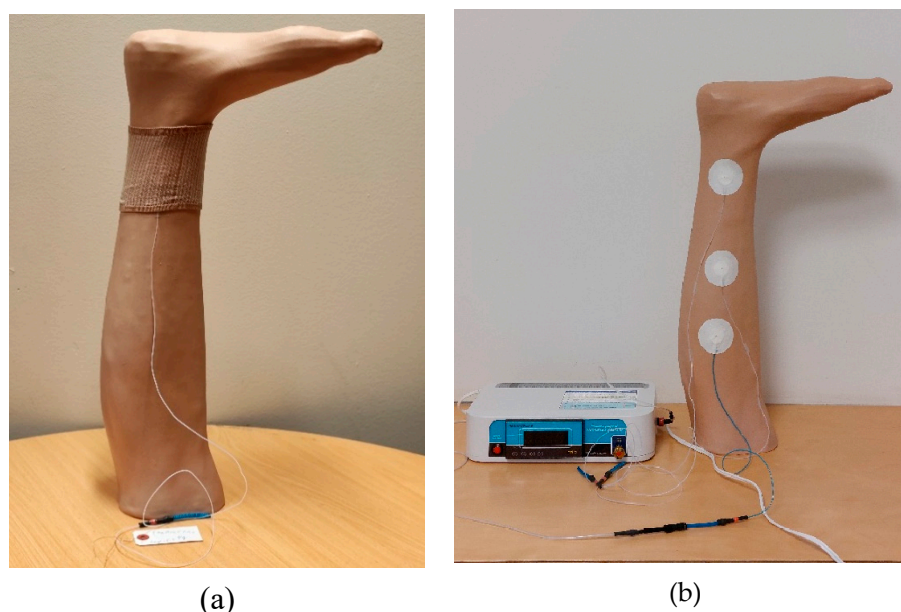


Figure 1. Evaluation of the pressure of knitted sample L1 by AMI air-pack pressure sensor at the ankle.

2.3. Statistical Analysis

The experimental data was analysed using SPSS software. Pearson correlation analysis was performed to examine the relationships among all variables. Multivariate analysis of variance (MANOVA) was conducted to evaluate the effects of loop length, number of yarns, and yarn materials on the material properties of the seamless punch-lace knitted fabrics. Prior to the analyses, the data were assessed for normality using measures of skewness and kurtosis, as well as histograms and normal Q-Q plots. The level of statistical significance was set at $\alpha = 0.05$.

3. Results and Discussion

3.1. Stretchability

MANOVA results indicate that the number of yarns has a significant effect on maximum load in both the weft (Yarn A: $F = 367.506$, $p < .001$; Yarn B: $F = 696.897$, $p < .001$; Yarn C: $F = 201.090$, $p < .001$) and warp directions (Yarn A: $F = 538.231$, $p < .001$; Yarn B: $F = 1062.547$, $p < .001$; Yarn C: $F = 141.771$, $p < .001$), whereas loop length and yarn material show no significant effects. A significant relationship was observed between fabric growth in the weft direction and loop length ($F = 26.545$, $p < .001$), as well as the number of Yarn D ($F = 5.792$, $p = .026$). Fabric growth in the warp direction was significantly influenced by the number of Yarn C ($F = 5.848$, $p = .025$). Pearson correlation analysis shows that maximum load in the weft and warp directions is almost perfectly correlated ($r = 0.992$, $p < .001$), indicating that they measure essentially the same property. Maximum load in both directions exhibits moderate negative correlations with the number of Yarn A (Weft: $r = -0.535$, $p = .007$; Warp: $r = -0.553$, $p = .005$) and very strong positive correlations with the number of Yarn B (Weft: $r = 0.910$, $p < .001$; Warp: $r = 0.953$, $p < .001$). Fabric growth in the weft direction is strongly positively correlated with loop length ($r = 0.772$, $p < .001$) and strongly negatively correlated with the number of Yarn C ($r = -0.658$, $p < .001$). Fabric growth in the warp direction shows a moderate positive correlation only with fabric growth in the weft direction ($r = 0.422$, $p = .040$).

Tensile stress-strain curves (Figure 2) show that a steeper slope indicates a higher tensile modulus and greater fabric stiffness. A similar trend is observed in both the weft and warp directions for the punch-lace knitted fabrics. Regarding the effect of loop length, L4 has the smallest loop length and the highest tensile modulus, followed by L3 and L2. This indicates that fabrics with smaller loop lengths possess greater strength and resistance to extension in both directions. This observation is consistent with the pressure measurements, where L4 exhibits higher pressure than L3 and L2. These

findings suggest that smaller loop lengths increase fabric stiffness and consequently provide higher compression to the wearer.

Considering the effect of yarn number, S2 and L2 exhibit higher tensile modules than S1 and L1, respectively, in the weft direction. This indicates that the addition of two ends of Yarn C in S2 and L2 reinforces the fabric structure and increases resistance to extension in the weft direction. In the warp direction, S2 displays a less steep stress–strain curve than S1 at low strain (up to approximately 10%), after which the curve becomes steeper. This behaviour may be attributed to the additional two ends of Yarn C, which slightly reduce the initial fabric length in the warp direction after knitting. As the fabric extends beyond 10% strain, the additional yarn begins to restrict further extension, requiring greater force. With respect to yarn materials, S3 exhibits a higher tensile modulus than L1 under the same loop length and also produces higher pressure. This indicates that 25D 77% nylon 23% spandex (Yarn D) enhances elastic resistance and compression compared with 43D 69% nylon 31% Lycra (Yarn A) used in L1.

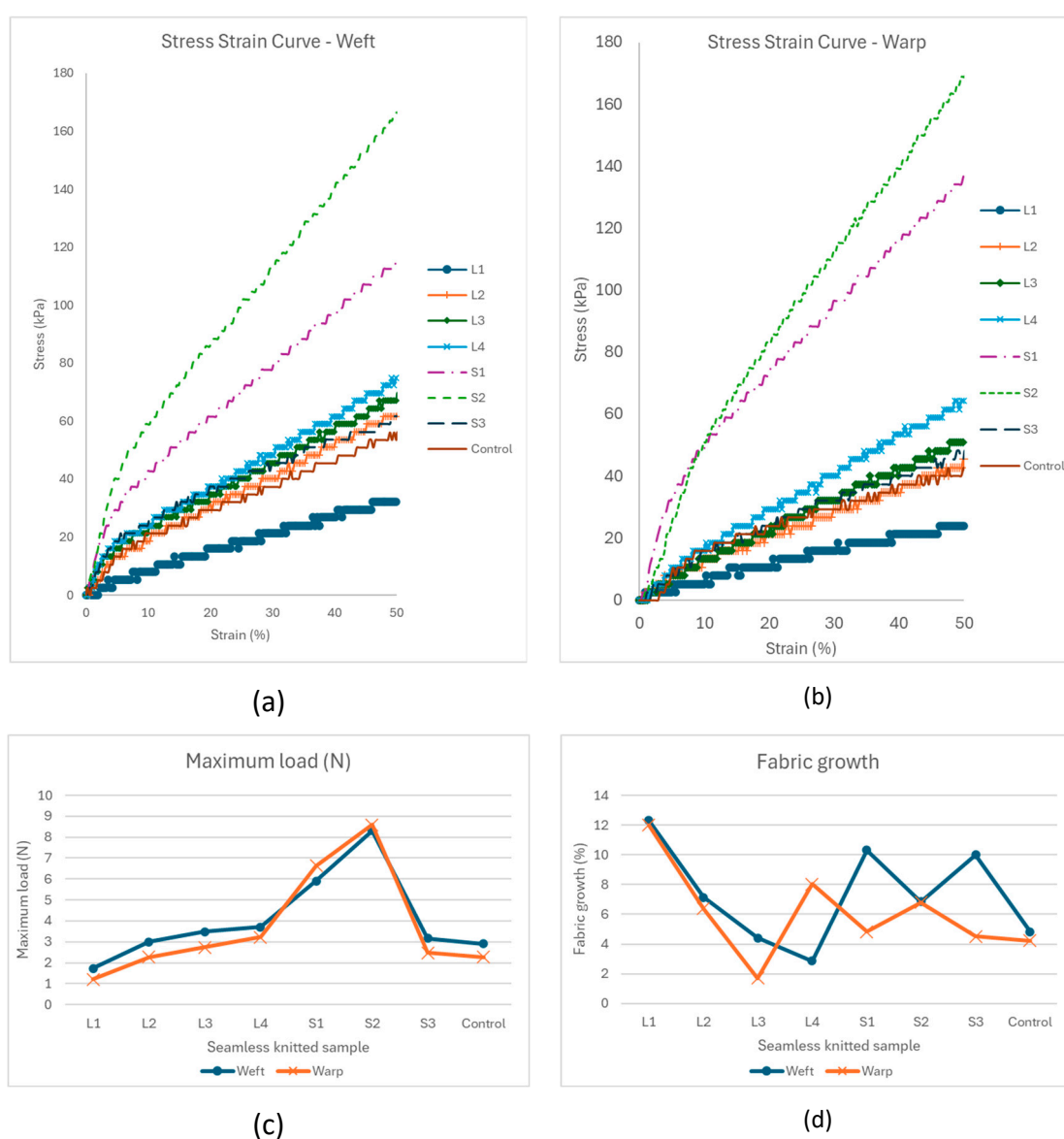


Figure 2. Tensile stress–strain curve of fabrics in the (a) weft and (b) warp direction; (c) maximum load (N); (d) fabric growth after 50% extension in the weft and warp direction.

Maximum load at 50% elongation represents the force required to extend the fabric to 50% of its original length; higher values indicate stronger and stiffer fabrics. Fabric S2 exhibits the highest maximum load, followed by S1 (Figure 2c). This suggests that the inclusion of 90D 86% nylon 14%

spandex (Yarn B) increases maximum load in both weft and warp directions. Under the same loop length conditions, the addition of two ends of 94 dtex 80% polyamide 6.6 20% Lycra (Yarn C) in S2 further strengthens the fabric structure, requiring greater force for extension in both directions.

Fabric growth represents the extent to which the fabric fails to return to its original length after extension. This parameter is critical for compression textiles, which are repeatedly stretched during wear; excessive growth may reduce pressure performance and shorten product lifespan. In the weft direction, fabric growth decreases as loop length decreases from 5.5 in L2 to 4.6 in L4 (Figure 2d). Stretchability in the weft direction is primarily governed by loop geometry (Figure 3a), as the knitted loop structure naturally facilitates extension. A smaller loop length results in a tighter structure, restricting yarn movement and stabilising the fabric, thereby improving recovery after extension.

A similar trend is observed for L1 and L2, and for S1 and S2. The addition of two ends of Yarn C in L2 and S2 reduces fabric growth compared with L1 and S1, respectively, in the weft direction. The extra yarn restricts loop movement and enhances the ability of the fabric to return to its original length after extension.

In the warp direction, fabric L4 exhibits greater growth than L3 and L2, despite having the smallest loop length. This may be attributed to the extension mechanism in the warp direction, which primarily stretches the loop head and leg (Figure 3). In tighter fabrics with smaller loop lengths, such as L4, the yarn experiences higher tensile tension for a given extension compared with looser fabrics such as L2, as the reduced loop geometry limits structural deformation and shifts the load to the yarn itself. This increases the likelihood of plastic deformation and incomplete recovery after extension.

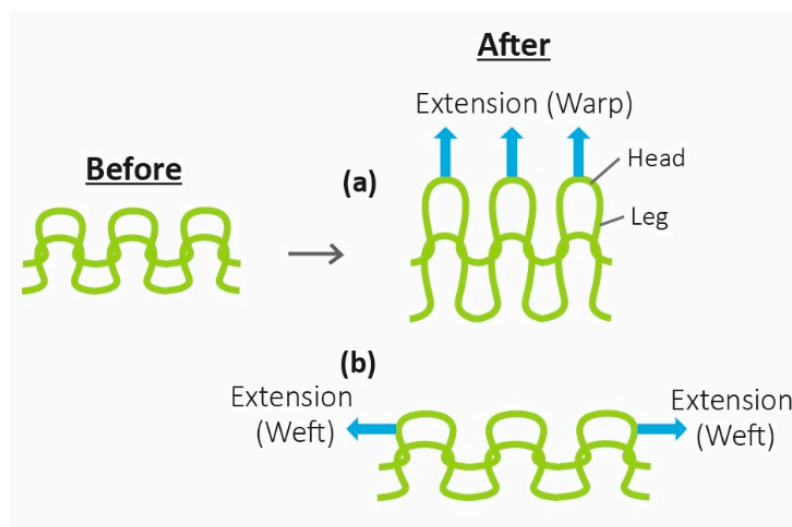


Figure 3. Loop movement during the extension in the (a) weft and (b) warp direction.

3.2. Pressure

Pearson correlation analysis revealed that pressure is strongly positively correlated with the number of Yarn B ($r = 0.849$, $p < .001$) and moderately negatively correlated with the number of Yarn A ($r = -0.516$, $p = .010$). Pressure also shows very strong positive correlations with maximum load in both the weft ($r = 0.932$, $p < .001$) and warp directions ($r = 0.934$, $p < .001$). However, no significant correlations were found between pressure and loop length or yarn material ($p > .05$). MANOVA results further indicate that the number of Yarn A ($F = 27.027$, $p < .001$), Yarn B ($F = 46.250$, $p < .001$), and Yarn C ($F = 8.277$, $p = .009$) significantly affect pressure.

Among the punch-lace fabrics shown in Figure 4, S2 exhibits the highest pressure at the ankle (26 mmHg), followed by S1 (23.17 mmHg) and L4 (21 mmHg). In terms of yarn number, both S1 and S2 produce higher pressures than the other fabric samples containing Yarns A and D, indicating that 90D 86% nylon 14% spandex (Yarn B) contributes substantially to increased compression in seamless knitted samples. The addition of two ends of 94 dtex 80% polyamide 6.6 20% Lycra (Yarn C) in S2

increased the pressure from 23.17 mmHg in S1 to 26 mmHg. However, L2 shows a pressure level similar to L1 despite the addition of two ends of Yarn C. This difference may be attributed to the varying yarn combinations in these fabric pairs. The addition of Yarn C appears to enhance fabric pressure when combined with Yarn B, but not when combined with Yarn A.

Comparing S3 and L1, S3 (19.33 mmHg) exhibits higher pressure than L1 (16.67 mmHg), indicating that 25D 77% nylon 23% spandex (Yarn D) provides greater compression than 43D 69% nylon 31% Lycra (Yarn A). Notably, fabric S1 (23.17 mmHg) produces approximately 35% higher pressure than the control fabric (17.17 mmHg) under the same loop length, demonstrating that the punch-lace structure incorporating two additional ends of 90D 86% nylon 14% spandex (Yarn B) significantly enhances compression performance.

Similar to the trend observed for maximum load in both the weft and warp directions (Figure 2c), measured pressure increases as loop length decreases from L2 to L4 (Figure 4). A smaller loop length results in a tighter structure and higher fabric stiffness. Stiffness describes the material's resistance to deformation under an applied force, particularly when the fabric expands due to muscle movement during wear. Increased stiffness, therefore, leads to higher applied pressure on the body and may also be interpreted as a greater change in compression per change in limb circumference [20,21]. This explains the strong positive correlations between pressure and maximum load in both the weft and warp directions. Fabrics with higher stiffness require greater force to extend and consequently exert higher compression pressure on the wearer.

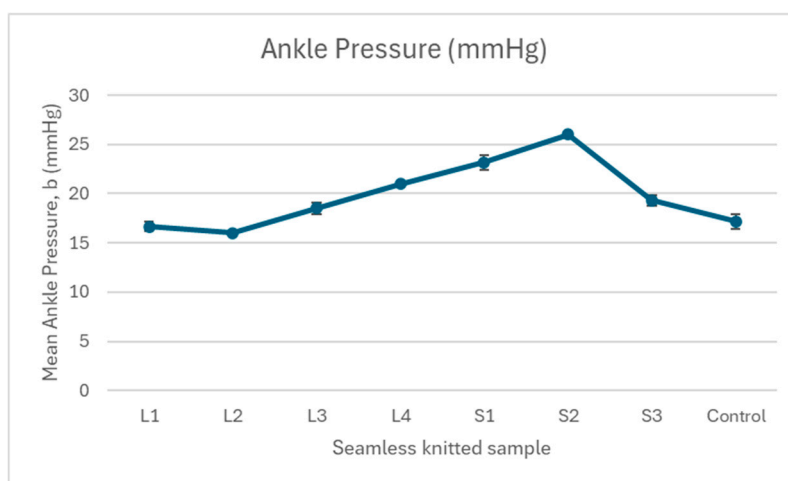


Figure 4. The pressure of the punch lace fabrics and the control fabric.

3.3. Air Permeability, Thermal Conductivity and Water Vapour Permeability

3.3.1. Air Permeability

For air permeability, lower ventilation resistance values indicate higher breathability and permeability. MANOVA results show significant effects of the number of Yarn A ($F = 631.45$, $p < .001$), B ($F = 126.76$, $p < .001$), and C ($F = 93.70$, $p < .001$), as well as yarn material ($F = 6.41$, $p < .05$), on ventilation resistance, whereas loop length has no significant effect

Pearson correlation analysis indicates a very strong positive correlation between ventilation resistance and the number of Yarn C ($r = 0.838$, $p < .001$). As shown in Figure 5, the addition of two extra ends of Yarn C in S2 and L2 results in higher ventilation resistance compared with S1 and L1, respectively. This suggests that additional Yarn C reduces air permeability, consistent with findings from our previous study [18]. This effect can be attributed to the increased fabric thickness and reduced porosity caused by the additional yarn, which restricts airflow through the fabric.

Regarding yarn material, L1 exhibits lower ventilation resistance than S3 (Figure 5), indicating that 43D 69% nylon 31% Lycra (Yarn A) provides better breathability than 25D 77% nylon 23% spandex (Yarn D) in S3.

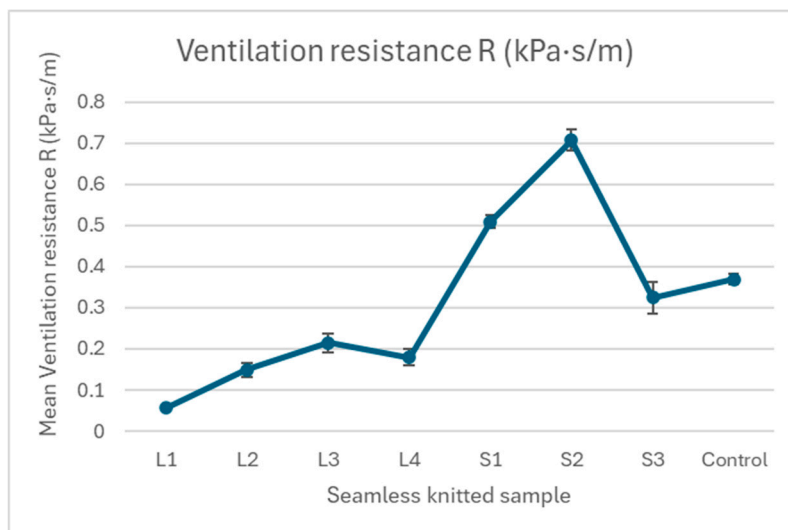


Figure 5. Ventilation resistance of the seamless punch lace knitted fabrics and the control fabric.

3.3.2. Thermal Conductivity

Pearson correlation analysis shows that thermal conductivity is strongly positively correlated with ventilation resistance ($r = 0.722$, $p < .001$). Among the seamless knitted samples, fabric S2 exhibits the highest thermal conductivity and ventilation resistance, followed by S1 and L3. This indicates that while S2 transfers heat more efficiently, it is less breathable.

Similar to air permeability, MANOVA results indicate that thermal conductivity is significantly influenced by the number of yarns A ($F = 36.31$, $p < .001$), B ($F = 40.26$, $p < .001$), C ($F = 5.58$, $p < .05$) and D ($F = 7.23$, $p < .05$), as well as yarn material ($F = 40.50$, $p < .001$), whereas loop length has no significant effect ($p > .05$). Thermal conductivity increases as the number of Yarn C increases, for example from two ends in L1 to four ends in L2, with a similar trend observed between S1 and S2 (Figure 6). This may be explained by the additional yarn providing a larger contact surface for heat transfer through conduction, thereby increasing thermal conductivity despite the increase in fabric thickness. These findings are consistent with our previous study [18].

With respect to yarn material, L1 shows thermal conductivity values similar to S3, suggesting that Yarns A and D have comparable effects on heat transfer. Since loop length does not significantly influence thermal conductivity, the higher values observed in S1 and S2 compared with L1 and L2 indicate that the inclusion of 90D 86% nylon 14% spandex (Yarn B) contributes more to thermal conductivity than 43D 69% nylon 31% Lycra (Yarn A). This may be attributed to the higher spandex content facilitating conductive heat transfer compared with Lycra. Consequently, fabrics knitted with Yarn B may dissipate heat more efficiently and potentially enhance thermal comfort compared with those knitted with Yarn A. Overall, the findings confirm that yarn material and yarn quantity are key factors influencing fabric thermal conductivity.

Interestingly, the control fabric exhibits the highest thermal conductivity, comparable to that of S2. Although S2 and the control fabric share the same loop length, S2 has greater thickness (1.77 mm) and areal density (452.24 g/m^2) than the control fabric (1 mm thickness; 242.45 g/m^2). S2 also contains two additional ends of Yarns B and C compared with the control. Despite these structural differences, the punch-lace fabric in S2 achieves a similar level of conductive heat transfer to the single-jersey control fabric. This suggests that the yarn combination used in S2 enables punch lace knitted fabrics to provide comparable thermal conductivity and therefore thermal comfort to conventional single jersey structures.

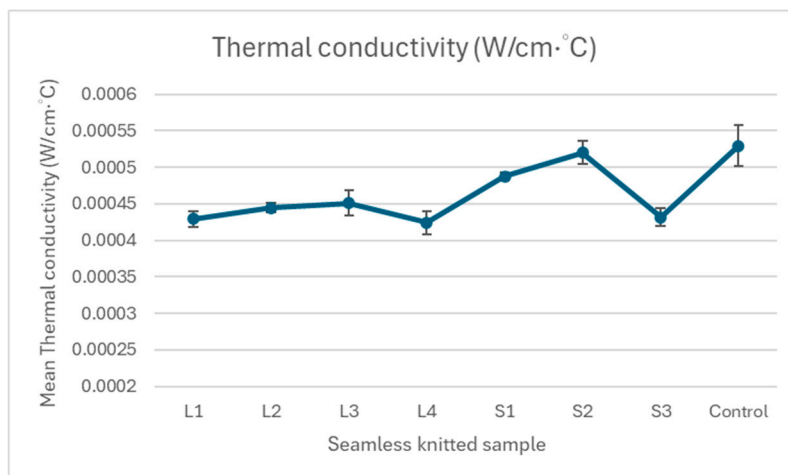


Figure 6. Thermal conductivity of the seamless punch lace knitted fabrics and the control fabric.

3.3.3. Water Vapour Permeability

Pearson correlation analysis shows no significant relationships between water vapour permeability and loop length, number of yarns, or yarn material in this study ($p > .05$). As shown in Figure 7, all seamless knitted fabrics and the control fabric exhibit similar water vapour permeability values. This suggests that factors beyond those investigated in this study may influence water vapour permeability, and further research is required to identify the key determinants of moisture transfer in compression textiles.

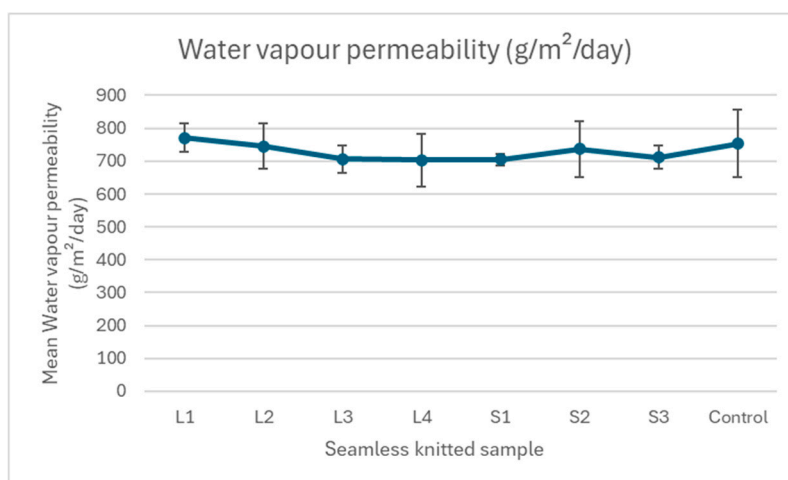


Figure 7. Water vapour permeability of seamless punch lace knitted fabrics and the control fabric.

3.4. Surface Friction and Roughness

MANOVA results indicate that the number of yarns, yarn materials, and loop length significantly influence the surface properties of seamless knitted fabrics in both the warp and weft directions ($p < .05$). In general, increasing the number of Yarn C from two ends in L1 to four ends in L2, and from two ends in S1 to four ends in S2 leads to higher MIU and SMD values in both directions, indicating increased surface friction and roughness (Table 5 and Figure 8).

Among the samples, S1 shows lower MIU and SMD values on average across different directions and fabric faces, suggesting that this fabric exhibits lower friction and a smoother surface. Pearson correlation analysis further reveals that surface roughness on the fabric face in the warp direction has a very strong negative correlation with ventilation resistance ($r = -0.789$, $p < .001$). This suggests that fabrics with lower air permeability tend to exhibit smoother surfaces in the warp direction.

This relationship may be explained by the fact that smoother fabric surfaces are typically produced by tighter loop structures and finer yarns, often achieved using finer-gauge knitting machines. These conditions create a denser and more compact fabric structure with reduced pore size and porosity, which restricts airflow through the fabric and consequently lowers air permeability. Fabric smoothness is an important factor influencing wearer comfort and may have long-term implications for treatment compliance when used in medical compression applications.

Table 5. Surface properties of seamless punch lace knitted fabrics and the control fabric.

	Surface Friction (MIU)				Surface Roughness (SMD)			
	Warp		Weft		Warp		Weft	
	Face	Back	Face	Back	Face	Back	Face	Back
L1	0.23	0.33	0.30	0.26	3.15	6.75	5.81	4.98
L2	0.23	0.30	0.31	0.27	3.43	8.80	9.38	5.53
L3	0.24	0.28	0.30	0.25	3.55	9.48	12.35	7.28
L4	0.26	0.28	0.31	0.26	3.52	7.84	12.42	6.32
S1	0.21	0.27	0.28	0.24	3.31	8.05	4.82	5.81
S2	0.23	0.25	0.29	0.26	3.32	8.25	8.58	6.26
S3	0.27	0.30	0.27	0.28	2.66	8.46	8.46	8.02
Control	0.28	0.27	0.26	0.31	3.01	4.25	2.90	3.77



Figure 8. Surface friction (MIU) of seamless punch lace knitted fabrics and the control fabric in (a) warp and (b) weft direction; surface roughness (SMD) of seamless punch lace knitted fabrics and the control fabric in (c) warp and (d) weft direction.

4. Conclusions

This study examined the effects of yarn material, number of yarns, and loop length on the mechanical and thermo-physiological properties of seamless punch-lace knitted fabrics for

compression applications. The number of yarns is the primary factor affecting the maximum load in both weft and warp directions, while loop length and yarn material show no significant direct effects. Smaller loop lengths and the inclusion of Yarn C improve dimensional recovery by restricting loop deformation.

Compression pressure is strongly associated with fabric stiffness and maximum load. Increasing yarn number, particularly Yarn B, significantly enhances pressure, while tighter loop structures indirectly contribute by increasing stiffness. Test results shows that air permeability decreases with increasing yarn number, especially Yarn C, due to increased fabric thickness and reduced porosity. Yarn A provides better breathability than Yarn D. In addition, thermal conductivity is mainly influenced by yarn number and yarn material and is positively related to ventilation resistance, indicating a trade-off between heat transfer and breathability. Surface properties are significantly affected by yarn number, yarn material, and loop length. Denser structures generally produce smoother surfaces but lower air permeability.

Among the tested samples, fabric S2 demonstrates the most promising performance for compression applications, exhibiting high pressure, good dimensional stability, smooth surface characteristics, and high thermal conductivity, although with reduced air permeability. Overall, yarn combination and structural parameters must be carefully balanced when designing seamless compression textiles, as improvements in pressure and mechanical stability may compromise breathability and thermal comfort.

Author Contributions: Conceptualization, N.W.L.; methodology, N.W.L., and M.-Y.K.; software, N.W.L., and K.-L.Y.; validation, N.W.L.; formal analysis, N.W.L.; investigation, N.W.L., and M.-Y.K.; resources, N.W.L., and K.-L.Y.; data curation, N.W.L., and M.-Y.K.; writing—original draft preparation, N.W.L.; writing—review and editing, N.W.L., M.-Y.K., and K.-L.Y.; visualization, N.W.L.; supervision, N.W.L.; project administration, N.W.L.; funding acquisition, N.W.L. All authors have read and agreed to the published version of the manuscript.

Funding: This project is supported by the University of Technology Sydney (UTS) under the UTS Collaboration Scheme (Project code: PRO23-17450) and the Faculty of Design and Society (FDS) under the 2023 DAB Research Support Scheme.

Institutional Review Board Statement: Not applicable.

Data Availability Statement: The original contributions presented in this study are included in the article. Further inquiries can be directed to the corresponding author.

Acknowledgments: The authors thank UTS and FDS for supporting this project.

Conflicts of Interest: The authors declare no conflicts of interest.

References

1. Morales Cuenca, G., F. Abadia Sanchez, and J.L. Aguayo Albasini, *What to do (or what «not to do») to increase the use of graduated compression stockings in patients with chronic venous disease?* *Cirugia española (English ed.)*, 2022. **100**(8): p. 522-524.
2. Coelho Rezende, G., B. O'Flynn, and C. O'Mahony, *Smart Compression Therapy Devices for Treatment of Venous Leg Ulcers: A Review*. *Advanced healthcare materials*, 2022. **11**(17): p. 1-19.
3. Nakashima, N., et al., *Compression Stockings Improve Lower Legs Symptom in Patients with Pulmonary Artery Hypertension Treated by Pulmonary Vasodilators-A Pilot Study*. *Journal of clinical medicine*, 2023. **12**(7): p. 2484.
4. Sanchez Jimenez, J.L., et al., *The Review of compression stocking in sports market*. *European Journal of Human Movement*, 2024. **53**(53): p. 5-31.
5. Mota, G.R., et al., *Effects of Wearing Compression Stockings on Exercise Performance and Associated Indicators: A Systematic Review*. *Open access journal of sports medicine*, 2020. **11**: p. 29-42.
6. Lee, D.C.W., et al., *Wearing Compression Garment Enhances Central Hemodynamics? A Systematic Review and Meta-Analysis*. *Journal of strength and conditioning research*, 2022. **36**(8): p. 2349-2359.

7. O'Riordan, S.F., et al., *Sports compression garments improve resting markers of venous return and muscle blood flow in male basketball players*. *Journal of sport and health science*, 2023. **12**(4): p. 513-522.
8. Franke, T.P.C., F.J.G. Backx, and B.M.A. Huisstede, *Lower extremity compression garments use by athletes: why, how often, and perceived benefit*. *BMC sports science, medicine & rehabilitation*, 2021. **13**(1): p. 31-14.
9. Pérez-Soriano, P., et al., *Influence of compression sportswear on recovery and performance: A systematic review*. *Journal of industrial textiles*, 2019. **48**(9): p. 1505-1524.
10. Brubacher, K., R.M. Rossi, and N. Kankariya, *Efficacy of Compression Garments in Medical and Sports Applications*, in *Compression Textiles for Medical, Sports, and Allied Applications*. 2024, CRC Press: United Kingdom. p. 139-156.
11. Kankariya, N., *Material, structure, and design of textile-based compression devices for managing chronic edema*. *Journal of Industrial Textiles*, 2022. **52**.
12. Xiong, Y. and X. Tao, *Compression Garments for Medical Therapy and Sports*. *Polymers*, 2018. **10**(6): p. 663.
13. Zadekhast, R. and A. Asayesh, *The Effect of Fabric Structure on the Compression Behavior of Rib Weft Knitted Fabrics*. *Fibers and polymers*, 2021. **22**(10): p. 2878-2884.
14. Chattopadhyay, R., R.M. Rossi, and N. Kankariya, *Materials and Structure of Compression Bandages and Stocking Devices*. 2024, CRC Press: United Kingdom. p. 15-30.
15. Lozo, M., et al., *Designing compression of preventive compression stockings*. *Journal of engineered fibers and fabrics*, 2021. **16**.
16. Sarı, B. and N. Oğlakcioğlu, *Analysis of the parameters affecting pressure characteristics of medical stockings*. *Journal of industrial textiles*, 2018. **47**(6): p. 1083-1096.
17. Li, N.-W., et al., *Mechanical and Thermal Behaviours of Weft-Knitted Spacer Fabric Structure with Inlays for Insole Applications*. *Polymers*, 2022. **14**(3): p. 619.
18. Li, N.W., M.-Y. Kwan, and K.-L. Yick, *Pressure and Thermal Behavior of Elastic Polyurethane and Polyamide Knitted Fabrics for Compression Textiles*. *Polymers*, 2025. **17**(7): p. 831.
19. Li, N.W., M.-y. Kwan, and K.-l. Yick, *Graduated compression stocking performance: Insights from wearers and development of a cost-effective 3D-printed leg mannequin*. *Textile Research Journal*, 2024. **0**(0): p. 00405175241297170.
20. Partsch, H., et al., *The Static Stiffness Index: an important parameter to characterise compression therapy in vivo*. *Journal of wound care*, 2016. **25**(Sup9): p. S4-S10.
21. Kisiel, M., et al., *Stiffness in compression therapy: Analytical estimation of pressure changes beneath textile compression devices*. *Textile research journal*, 2025. **95**(5-6): p. 599-610.

Disclaimer/Publisher's Note: The statements, opinions and data contained in all publications are solely those of the individual author(s) and contributor(s) and not of MDPI and/or the editor(s). MDPI and/or the editor(s) disclaim responsibility for any injury to people or property resulting from any ideas, methods, instructions or products referred to in the content.